# Development of a fuel depletion sensitivity calculation module for multi-cell problems in a deterministic reactor physics code system CBZ

Go Chiba*,[a], Yosuke Kawamoto[a], Tadashi Narabayashi[a]

[a] *Hokkaido University, Kita-ku, Sapporo, Hokkaido 060-8628, Japan*

**Abstract**

A new functionality of fuel depletion sensitivity calculations is developed as one module in a deterministic reactor physics code system CBZ. This is based on the generalized perturbation theory for fuel depletion problems. The theory for fuel depletion problems with a multi-layer depletion step division scheme is described in detail. Numerical techniques employed in actual implementation are also provided. Verification calculations are carried out for a 3×3 multi-cell problem consisting of two different types of fuel pins. It is shown that the sensitivities of nuclide number densities after fuel depletion with respect to the nuclear data calculated by the new module agree well with reference sensitivities calculated by direct numerical differentiation. To demonstrate the usefulness of the new module, fuel depletion sensitivities in different multi-cell arrangements are compared and non-negligible differences are observed. Nuclear data-induced uncertainties of nuclide number densities obtained with the calculated sensitivities are also compared.

*Key words:* uncertainty quantification, generalized perturbation theory, fuel depletion

## 1. Introduction

Accurate and reliable prediction of nuclide number densities after fuel depletion is quite important in various applications in the field of nuclear engineering, including safety analyses of nuclear power plants and nuclear waste fuel management. Since safety margins, which should be considered for various functionalities of nuclear systems, significantly affect construction and operation costs, an important issue is the quantitative evaluation of accuracy and reliability. Uncertainty quantification (UQ) is one of promising ways to fulfill this requirement; much research and development of UQ has been conducted to date in the field of reactor physics.

One of numerical procedures for UQ is the adjoint-based method, in which sensitivities of observed (target) parameters with respect to input parameters that include uncertainties are calculated and input parameter-induced uncertainties are evaluated by manipulation of the sensitivities and uncertainty information on the input parameters. In the field of reactor physics, the perturbation theory and the generalized

*Corresponding author, Tel: +81-10-706-6683, Fax: +81-10-706-6683
*Email address:* go_chiba@eng.hokudai.ac.jp (Go Chiba)

perturbation theory (GPT) are well established and implemented to application codes to calculate the sensitivities of reactor physics parameters with respect to nuclear data, which is a principal source of uncertainty. Fuel depletion problems for heterogeneous systems are complicated because they are coupled problems between fuel depletion and neutron transport problems. A theory for these problems, GPT for fuel depletion problems, however, has been established(Williams, 1979; Takeda, 1985). While this theory exists, actual implementation to lattice physics codes is quite rare.

A deterministic reactor physics code system CBZ, which has been under development at Hokkaido University in Japan, has various functionalities for UQ, including fuel depletion problems for a single fuel pin cell. In order to enhance this capability, a new fuel depletion sensitivity calculation module has been developed and implemented. The purpose of the present paper is to describe this new CBZ functionality.

The present paper is organized as follows: Section 2 describes the generalized perturbation theory for fuel depletion problems and actual implementation. Sections 3 and 4 are devoted, respectively, to the description of numerical procedures and results. Finally, Section 5 provides the conclusions of the present study and future perspectives.

## 2. Theory and implementation

### *2.1. General description of fuel depletion calculations*

Generally in fuel depletion calculations, the fuel depletion period is divided into *steps* and each of the steps is further divided into *sub-steps*. In the frame of the deterministic numerical procedure, resonance self-shielding and neutron flux calculations are carried out at the beginning of each step; and the calculated multi-group cross sections and neutron flux distributions are commonly used during each step. At the beginning of each sub-step, neutron flux distribution is normalized and fuel depletion during the sub-step is calculated with the normalized neutron flux.

Let us consider a step which is divided into $I$ sub-steps. The beginning and end of sub-step $i$ are denoted as $t_i$ and $t_{i+1}$, while the beginning and end of this step are denoted as $t_0$ and $t_I$. Note that sub-steps are denoted as $0, 1, ..., I-1$.

Neutron flux distribution $\Phi$ at a particular step is defined as the solution to the following neutron transport equation:

$$\mathbf{B}_0\Phi = \left(\mathbf{A}_0 - \frac{1}{k_{\mathrm{eff},0}}\mathbf{F}_0\right)\Phi = 0, \tag{1}$$

where $k_{\mathrm{eff}}$ is the effective neutron multiplication factor, and $\mathbf{A}$ and $\mathbf{F}$ are operators for neutron loss and production, respectively. The subscript for $k_{\mathrm{eff}}$ and the operators describes the time at which these are

defined. The neutron flux distribution $\Phi$ is normalized by the following equation:

$$\langle \nu \Sigma_{f,0} \Phi \rangle = \text{Const.} \tag{2}$$

Neutron flux distribution at sub-step $i$, $\phi_i$, is assumed to be proportional to $\Phi$ and is defined as

$$\phi_i = f_i \Phi. \tag{3}$$

The normalization factor $f_i$ is defined so as to satisfy the following equation:

$$\mathbf{G}_i \phi_i = f_i \mathbf{G}_i \Phi = P, \tag{4}$$

where $\mathbf{G}_i$ is an operator for the normalization at sub-step $i$ and $P$ denotes values of the normalization. We denote average of energy-integrated value for $\Phi$ (average total neutron flux) in a fuel region $j$ as $\tilde{\Phi}^j$, which is defined as

$$\tilde{\Phi}^j = \frac{\int dE \int_{\mathbf{r} \in j} \Phi(\mathbf{r}, E) d\mathbf{r}}{\int_{\mathbf{r} \in j} d\mathbf{r}}. \tag{5}$$

Total neutron flux in a region $j$ at sub-step $i$, $\tilde{\phi}_i^j$, can be written as

$$\tilde{\phi}_i^j = f_i \tilde{\Phi}^j. \tag{6}$$

Let us assume that we consider a system in which there are $J$ fuel regions.

A number density vector in a region $j$ at time $t$ is denoted as $\mathbf{N}^j(t)$. The number density vectors at $t_0$, $\mathbf{N}^j(t_0)$, are given as an initial condition. The fuel depletion equation in this region at sub-step $i$ is written as

$$\frac{d\mathbf{N}^j(t)}{dt} = \mathbf{M}_i^j \mathbf{N}^j(t), \qquad (t_i \leq t < t_{i+1}). \tag{7}$$

The fuel depletion matrix in a region $j$ at sub-step $i$, $\mathbf{M}_i^j$, can be decomposed as follows:

$$\mathbf{M}_i^j = \mathbf{M}_\lambda + \mathbf{M}_\phi^j \tilde{\phi}_i^j = \mathbf{M}_\lambda + \mathbf{M}_\phi^j f_i \tilde{\Phi}^j, \tag{8}$$

where $\mathbf{M}_\lambda$ and $\mathbf{M}_\phi$ are fuel depletion matrix components for radioactive decay and neutron-nuclide reaction. Note that entries of $\mathbf{M}_\phi$ are composed of the one-group cross sections.

A fuel depletion equation for the whole system at sub-step $i$ is written as

$$\frac{d\mathbf{N}(t)}{dt} = \frac{d}{dt} \begin{pmatrix} \mathbf{N}^1(t) \\ \mathbf{N}^2(t) \\ \vdots \\ \mathbf{N}^J(t) \end{pmatrix} = \begin{pmatrix} \mathbf{M}_i^1 & \mathbf{0} & \cdots & \mathbf{0} \\ \mathbf{0} & \mathbf{M}_i^2 & \cdots & \mathbf{0} \\ \vdots & \vdots & \ddots & \cdots \\ \mathbf{0} & \mathbf{0} & \cdots & \mathbf{M}_i^J \end{pmatrix} \begin{pmatrix} \mathbf{N}^1(t) \\ \mathbf{N}^2(t) \\ \vdots \\ \mathbf{N}^J(t) \end{pmatrix} = \mathbf{M}_i \mathbf{N}(t), \qquad (t_i \leq t < t_{i+1}). \tag{9}$$

### 2.2. Generalized perturbation theory for fuel depletion problems

Although several papers on GPT for fuel depletion problems have been published and the theoretical detail of GPT has well been documented(Williams, 1979; Takeda, 1985), there are none that explicitly describe GPT for fuel depletion problems with a multi-layer depletion step division scheme consisting of depletion steps and sub-steps.

Let us focus on the number density of nuclide $k$ in region $j$ after fuel depletion, $N_k^j(t_I)$. The sensitivity of this quantity with respect to arbitrary nuclear data $\sigma$ is defined as

$$S = \frac{\sigma}{N_k^j(t_I)} \frac{dN_k^j(t_I)}{d\sigma} = \frac{\sigma}{N_k^j(t_I)} \mathbf{e}_{(j-1)\times K+k}^T \frac{d\mathbf{N}(t_I)}{d\sigma}, \tag{10}$$

where $\mathbf{e}_j$ is a vector in which the $j$th entry is unity and others are zero, and $K$ denotes the number of nuclides in each fuel region. The superscript $T$ for vectors and matrices is for the transposition.

In order to calculate $\frac{dN_k^j(t_I)}{d\sigma}$ in Eq. (10), a vector $\mathbf{w}(t)$, whose size is the same as that of $\mathbf{N}$, is multiplied to both sides of Eq. (9), both the sides are integrated over the entire period $[t_0, t_I]$, and then the following equation is derived.

$$\begin{aligned}
\int_{t_0}^{t_I} \mathbf{w}^T \frac{d\mathbf{N}}{dt} dt &= \sum_{i=0}^{I-1} \int_{t_i}^{t_{i+1}} \mathbf{w}^T \mathbf{M}_i \mathbf{N} dt, \\
\left[\mathbf{w}^T \mathbf{N}\right]_{t_0}^{t_I} &= \int_{t_0}^{t_I} \frac{d\mathbf{w}^T}{dt} \mathbf{N} dt + \sum_{i=0}^{I-1} \int_{t_i}^{t_{i+1}} \mathbf{w}^T \mathbf{M}_i \mathbf{N} dt, \\
\mathbf{w}^T(t_I)\mathbf{N}(t_I) &= \mathbf{w}^T(t_0)\mathbf{N}(t_0) + \int_{t_0}^{t_I} \frac{d\mathbf{w}^T}{dt} \mathbf{N} dt + \sum_{i=0}^{I-1} \int_{t_i}^{t_{i+1}} \mathbf{w}^T \mathbf{M}_i \mathbf{N} dt.
\end{aligned} \tag{11}$$

For simplicity, dependence of $\mathbf{N}$ and $\mathbf{w}$ on time in integrations is omitted. Setting

$$\mathbf{w}(t_I) = \mathbf{e}_{(j-1)\times K+k}, \tag{12}$$

as the final condition of $\mathbf{w}(t)$, $N_k^j(t_I)$ can be written as

$$N_k^j(t_I) = \mathbf{w}^T(t_0)\mathbf{N}(t_0) + \int_{t_0}^{t_I} \frac{d\mathbf{w}^T}{dt} \mathbf{N} dt + \sum_{i=0}^{I-1} \int_{t_i}^{t_{i+1}} \mathbf{w}^T \mathbf{M}_i \mathbf{N} dt. \tag{13}$$

By differentiating both sides of Eq. (13) by $\sigma$, the following equation is derived:

$$\frac{dN_k^j(t_I)}{d\sigma} = \int_{t_0}^{t_I} \frac{d\mathbf{w}^T}{dt} \frac{d\mathbf{N}}{d\sigma} dt + \sum_{i=0}^{I-1} \int_{t_i}^{t_{i+1}} \mathbf{w}^T \frac{d\mathbf{M}_i}{d\sigma} \mathbf{N} dt + \sum_{i=0}^{I-1} \int_{t_i}^{t_{i+1}} \mathbf{w}^T \mathbf{M}_i \frac{d\mathbf{N}}{d\sigma} dt. \tag{14}$$

The first and third terms in the right hand side (RHS) of Eq. (14) disappear if the vector $\mathbf{w}$ is properly defined as described later.

Let us consider the second term in the RHS of Eq. (14). This can be rewritten as

$$\sum_{i=0}^{I-1}\int_{t_i}^{t_{i+1}}\mathbf{w}^T\frac{d\mathbf{M}_i}{d\sigma}\mathbf{N}dt=\sum_{i=0}^{I-1}\sum_{j=1}^{J}\int_{t_i}^{t_{i+1}}\mathbf{w}^{jT}\frac{d\mathbf{M}_i^j}{d\sigma}\mathbf{N}^j dt$$
$$=\sum_{i=0}^{I-1}\sum_{j=1}^{J}\int_{t_i}^{t_{i+1}}\mathbf{w}^{jT}\frac{\partial\mathbf{M}_i^j}{\partial\sigma}\mathbf{N}^j dt+\sum_{i=0}^{I-1}\sum_{j=1}^{J}\sum_{g}\frac{d\tilde{\Phi}_g^j}{d\sigma}\int_{t_i}^{t_{i+1}}\mathbf{w}^{jT}\frac{\partial\mathbf{M}_i^j}{\partial\tilde{\Phi}_g^j}\mathbf{N}^j dt+\sum_{i=0}^{I-1}\sum_{j=1}^{J}\int_{t_i}^{t_{i+1}}\mathbf{w}^{jT}\frac{df_i}{d\sigma}\frac{\partial\mathbf{M}_i^j}{\partial f_i}\mathbf{N}^j dt, \tag{15}$$

where $\tilde{\Phi}_g^j$ denotes average neutron flux of group $g$ in region $j$. The first term in the RHS of Eq. (15) corresponds to direct effect of nuclear data to fuel depletion matrix, and partial differentiation $\frac{\partial\mathbf{M}_i^j}{\partial\sigma}$ can be easily calculated. The second and third terms correspond to indirect effects of nuclear data to fuel depletion matrix via a neutron flux spatial and energy distributions and via a neutron flux normalization factors, respectively.

The second term in the RHS of Eq. (15) can be rewritten as

$$\sum_{i=0}^{I-1}\sum_{j=1}^{J}\sum_{g}\frac{d\tilde{\Phi}_g^j}{d\sigma}\int_{t_i}^{t_{i+1}}\mathbf{w}^{jT}\frac{\partial\mathbf{M}_i^j}{\partial\tilde{\Phi}_g^j}\mathbf{N}^j dt=\sum_{j=1}^{J}\sum_{g}\frac{d\tilde{\Phi}_g^j}{d\sigma}\sum_{i=0}^{I-1}\int_{t_i}^{t_{i+1}}\mathbf{w}^{jT}\frac{\partial\left(\mathbf{M}_\phi^j\tilde{\Phi}^j f_i\right)}{\partial\tilde{\Phi}_g^j}\mathbf{N}^j dt$$
$$=\sum_{j=1}^{J}\sum_{g}\frac{d\tilde{\Phi}_g^j}{d\sigma}\sum_{i=0}^{I-1}f_i\int_{t_i}^{t_{i+1}}\mathbf{w}^{jT}\mathbf{M}_{\phi,g}^j\mathbf{N}^j dt, \tag{16}$$

where

$$\mathbf{M}_{\phi,g}^j=\frac{\partial\left(\mathbf{M}_\phi^j\tilde{\Phi}^j\right)}{\partial\tilde{\Phi}_g^j}. \tag{17}$$

Since entries of the matrix $\mathbf{M}_\phi^j\tilde{\Phi}^j$ correspond to the reaction rates, the matrix $\mathbf{M}_{\phi,g}^j$ has non-zero entries which are related to the $g$th-group cross sections.

Next, let us consider the third term in the RHS of Eq. (15). By differentiating Eq. (4) by $\sigma$, the following equation can be derived:

$$\frac{df_i}{d\sigma}\frac{P}{f_i}+f_i\frac{d\mathbf{G}_i}{d\sigma}\Phi+f_i\mathbf{G}_i\frac{d\Phi}{d\sigma}=0. \tag{18}$$

Then we can obtain

$$\frac{df_i}{d\sigma}=-\frac{f_i^2}{P}\left(\frac{d\mathbf{G}_i}{d\sigma}\Phi+\mathbf{G}_i\frac{d\Phi}{d\sigma}\right). \tag{19}$$

With Eq.(19), the third term in the RHS of Eq. (15) can be rewritten as

$$\sum_{i=0}^{I-1}\sum_{j=1}^{J}\int_{t_i}^{t_{i+1}}\mathbf{w}^{jT}\frac{df_i}{d\sigma}\frac{\partial\mathbf{M}_i^j}{\partial f_i}\mathbf{N}^j dt=\sum_{i=0}^{I-1}\frac{df_i}{d\sigma}\sum_{j=1}^{J}\int_{t_i}^{t_{i+1}}\mathbf{w}^{jT}\left(\mathbf{M}_\phi^j\tilde{\Phi}^j\right)\mathbf{N}^j dt$$
$$=\sum_{i=0}^{I-1}\left(-\frac{f_i^2}{P}\right)\left(\frac{d\mathbf{G}_i}{d\sigma}\Phi+\mathbf{G}_i\frac{d\Phi}{d\sigma}\right)\sum_{j=1}^{J}\int_{t_i}^{t_{i+1}}\mathbf{w}^{jT}\left(\mathbf{M}_\phi^j\tilde{\Phi}^j\right)\mathbf{N}^j dt=-\sum_{i=0}^{I-1}f_i P_i^\dagger\left(\frac{d\mathbf{G}_i}{d\sigma}\Phi+\mathbf{G}_i\frac{d\Phi}{d\sigma}\right), \tag{20}$$

where

$$P_i^\dagger = \frac{\sum_{j=1}^{J}\int_{t_i}^{t_{i+1}} \mathbf{w}^{j\,T}\left(\mathbf{M}_\phi^j \tilde{\Phi}^j f_i\right)\mathbf{N}^j dt}{P}. \tag{21}$$

Also if we write

$$\mathbf{G}_i\Phi = \sum_{j=1}^{J} V^j \sum_g G_{i,g}^j \tilde{\Phi}_g^j, \tag{22}$$

the third term in the RHS of Eq. (15) can be written as

$$\sum_{i=0}^{I-1}\sum_{j=1}^{J}\int_{t_i}^{t_{i+1}} \mathbf{w}^{j\,T}\frac{df_i}{d\sigma}\frac{\partial \mathbf{M}_i^j}{\partial f_i}\mathbf{N}^j dt = -\sum_{i=0}^{I-1} f_i P_i^\dagger \left(\sum_{j=1}^{J} V^j \sum_g \frac{dG_{i,g}^j}{d\sigma}\tilde{\Phi}_g^j + \sum_{j=1}^{J} V^j \sum_g G_{i,g}^j \frac{d\tilde{\Phi}_g^j}{d\sigma}\right). \tag{23}$$

Note that $V^j$ denotes the volume of region $j$.

With Eqs. (15), (16) and (23), the second term in the RHS of Eq. (14) can be rewritten as

$$\begin{aligned}
\sum_{i=0}^{I-1}\int_{t_i}^{t_{i+1}} \mathbf{w}^T\frac{d\mathbf{M}_i}{d\sigma}\mathbf{N}dt &= \sum_{i=0}^{I-1}\sum_{j=1}^{J}\int_{t_i}^{t_{i+1}} \mathbf{w}^{j\,T}\frac{\partial \mathbf{M}_i^j}{\partial\sigma}\mathbf{N}^j dt + \sum_{j=1}^{J}\sum_g \frac{d\tilde{\Phi}_g^j}{d\sigma}\sum_{i=0}^{I-1} f_i \int_{t_i}^{t_{i+1}} \mathbf{w}^{j\,T}\mathbf{M}_{\phi,g}^j\mathbf{N}^j dt \\
&\quad - \sum_{i=0}^{I-1} f_i P_i^\dagger \left(\sum_{j=1}^{J} V^j \sum_g \frac{dG_{i,g}^j}{d\sigma}\tilde{\Phi}_g^j + \sum_{j=1}^{J} V^j \sum_g G_{i,g}^j \frac{d\tilde{\Phi}_g^j}{d\sigma}\right) \\
&= \sum_{i=0}^{I-1}\sum_{j=1}^{J}\int_{t_i}^{t_{i+1}} \mathbf{w}^{j\,T}\frac{\partial \mathbf{M}_i^j}{\partial\sigma}\mathbf{N}^j dt + \sum_g\sum_{j=1}^{J}\frac{d\tilde{\Phi}_g^j}{d\sigma}\left\{\sum_{i=0}^{I-1}\left(f_i\int_{t_i}^{t_{i+1}} \mathbf{w}^{j\,T}\mathbf{M}_{\phi,g}^j\mathbf{N}^j dt - V^j G_{i,g}^j f_i P_i^\dagger\right)\right\} \\
&\quad - \sum_{i=0}^{I-1} f_i P_i^\dagger \sum_{j=1}^{J} V^j \sum_g \frac{dG_{i,g}^j}{d\sigma}\tilde{\Phi}_g^j.
\end{aligned} \tag{24}$$

Next, let us consider the term $\dfrac{d\tilde{\Phi}_g^j}{d\sigma}$ in the RHS of Eq. (24). By differentiating both sides of the neutron transport Eq. (1) by $\sigma$, we can obtain

$$\left(\frac{\partial \mathbf{B}_0}{\partial\sigma} + \frac{\partial \mathbf{B}_0}{\partial \mathbf{N}^T(t_0)}\frac{d\mathbf{N}(t_0)}{d\sigma}\right)\Phi + \mathbf{B}_0\frac{d\Phi}{d\sigma} = 0. \tag{25}$$

At this point the following generalized adjoint equation to Eq. (1) is defined:

$$\mathbf{B}_0^\dagger\Gamma^\dagger = S^\dagger. \tag{26}$$

The superscript † is used to denote the adjoint operators and quantities. Boundary conditions for $\Gamma^\dagger$ should be properly chosen in accordance with those for $\Phi$. The generalized adjoint neutron flux $\Gamma^\dagger$ is multiplied to both sides of Eq. (25) and both the sides are integrated over whole energy and space. Then, the following

equation is derived:

$$\left\langle \Gamma^\dagger, \frac{\partial \mathbf{B}_0}{\partial \sigma}\Phi \right\rangle + \frac{d\mathbf{N}^T(t_0)}{d\sigma}\left\langle \Gamma^\dagger, \frac{\partial \mathbf{B}_0}{\partial \mathbf{N}(t_0)}\Phi \right\rangle + \left\langle \Gamma^\dagger, \mathbf{B}_0\frac{d\Phi}{d\sigma} \right\rangle$$
$$= \left\langle \Gamma^\dagger, \frac{\partial \mathbf{B}_0}{\partial \sigma}\Phi \right\rangle + \frac{d\mathbf{N}^T(t_0)}{d\sigma}\left\langle \Gamma^\dagger, \frac{\partial \mathbf{B}_0}{\partial \mathbf{N}(t_0)}\Phi \right\rangle + \left\langle \frac{d\Phi}{d\sigma}, \mathbf{B}_0^\dagger\Gamma^\dagger \right\rangle$$
$$= \left\langle \Gamma^\dagger, \frac{\partial \mathbf{B}_0}{\partial \sigma}\Phi \right\rangle + \frac{d\mathbf{N}^T(t_0)}{d\sigma}\left\langle \Gamma^\dagger, \frac{\partial \mathbf{B}_0}{\partial \mathbf{N}(t_0)}\Phi \right\rangle + \left\langle \frac{d\Phi}{d\sigma}S^\dagger \right\rangle = 0, \tag{27}$$

where the brackets $\langle\rangle$ denote the integration over whole energy and space. If the source $S^\dagger$ is given as flat over each region, the third term of Eq. (27) can be written as

$$\left\langle \frac{d\Phi}{d\sigma}S^\dagger \right\rangle = \sum_{j=1}^{J}\sum_g S_g^{j\dagger}\frac{d\tilde{\Phi}_g^j}{d\sigma}V^j. \tag{28}$$

If we define the source in Eq. (26) as

$$S_g^{j\dagger} = -\frac{1}{V^j}\left\{\sum_{i=0}^{I-1}\left(f_i\int_{t_i}^{t_{i+1}}\mathbf{w}^{j\,T}\mathbf{M}_{\phi,g}^j\mathbf{N}^j dt - V^j G_{i,g}^j f_i P_i^\dagger\right)\right\}, \tag{29}$$

the second term in the RHS of Eq. (24) can be written as

$$\sum_g\sum_{j=1}^{J}\frac{d\tilde{\Phi}_g^j}{d\sigma}\left\{\sum_{i=0}^{I-1}\left(f_i\int_{t_i}^{t_{i+1}}\mathbf{w}^{j\,T}\mathbf{M}_{\phi,g}^j\mathbf{N}^j dt - V^j G_{i,g}^j f_i P_i^\dagger\right)\right\}$$
$$= \left\langle \Gamma^\dagger, \frac{\partial \mathbf{B}_0}{\partial \sigma}\Phi \right\rangle + \sum_{j=1}^{J}\frac{d\mathbf{N}^{j\,T}(t_0)}{d\sigma}\left\langle \Gamma^\dagger, \frac{\partial \mathbf{B}_0}{\partial \mathbf{N}^j(t_0)}\Phi \right\rangle. \tag{30}$$

It is important to mention that the source $S^\dagger$ is orthogonal to the solution to the neutron transport Eq. (1), $\Phi$, and that the Fredholm alternative theorem guarantees non-zero solutions to Eq. (26).

Finally Eq. (14) can be written as

$$\frac{dN_k^j(t_I)}{d\sigma} = \sum_{j=1}^{J}\int_{t_0}^{t_I}\frac{d\mathbf{w}^{j\,T}}{dt}\frac{d\mathbf{N}^j}{d\sigma}dt + \sum_{i=0}^{I-1}\sum_{j=1}^{J}\int_{t_i}^{t_{i+1}}\mathbf{w}^{j\,T}\mathbf{M}_i^j\frac{d\mathbf{N}^j}{d\sigma}dt + \sum_{i=0}^{I-1}\sum_{j=1}^{J}\int_{t_i}^{t_{i+1}}\mathbf{w}^{j\,T}\frac{\partial \mathbf{M}_i^j}{\partial\sigma}\mathbf{N}^j dt$$
$$- \sum_{i=0}^{I-1}f_i P_i^\dagger\sum_{j=1}^{J}V^j\sum_g\frac{dG_{i,g}^j}{d\sigma}\tilde{\Phi}_g^j + \left\langle \Gamma^\dagger, \frac{\partial \mathbf{B}_0}{\partial \sigma}\Phi \right\rangle + \sum_{j=1}^{J}\frac{d\mathbf{N}^{j\,T}(t_0)}{d\sigma}\left\langle \Gamma^\dagger, \frac{\partial \mathbf{B}_0}{\partial \mathbf{N}^j(t_0)}\Phi \right\rangle. \tag{31}$$

Let us assume that $\mathbf{G}_i$ depends on $\mathbf{N}(t_i)$. In such a case, the term $\frac{d\mathbf{N}^j(t_i)}{d\sigma}$ should be considered in $\frac{dG_{i,g}^j}{d\sigma}$. In the following, we consider a case where the normalization is performed on the thermal output, for example. The normalization operator $G_{i,g}^j$ can be written as

$$G_{i,g}^j = \sum_k E_k N_k^j(t_i)\sigma_{f,k,g}^j = \mathbf{N}^{j\,T}(t_i)\mathbf{R}_g^j, \tag{32}$$

where $E_k$ denotes thermal energy per a fission reaction of nuclide $k$. From Eq. (32), the following equation can be derived:

$$\sum_{i=0}^{I-1} f_i P_i^\dagger \sum_{j=1}^{J} V^j \sum_g \frac{dG_{i,g}^j}{d\sigma} \tilde{\Phi}_g^j = \sum_{i=0}^{I-1} f_i P_i^\dagger \sum_{j=1}^{J} V^j \sum_g \frac{d\mathbf{N}^{j\,T}(t_i)}{d\sigma} \mathbf{R}_g^j \tilde{\Phi}_g^j + \sum_{i=0}^{I-1} f_i P_i^\dagger \sum_{j=1}^{J} V^j \sum_g \mathbf{N}^{j\,T}(t_i) \frac{d\mathbf{R}_g^j}{d\sigma} \tilde{\Phi}_g^j. \quad (33)$$

Inserting Eq. (33) into Eq. (31), we obtain

$$\begin{aligned} \frac{dN_k^j(t_I)}{d\sigma} = &\sum_{j=1}^{J} \int_{t_0}^{t_I} \frac{d\mathbf{w}^{j\,T}}{dt} \frac{d\mathbf{N}^j}{d\sigma} dt + \sum_{i=0}^{I-1} \sum_{j=1}^{J} \int_{t_i}^{t_{i+1}} \mathbf{w}^{j\,T} \mathbf{M}_i^j \frac{d\mathbf{N}^j}{d\sigma} dt + \sum_{i=0}^{I-1} \sum_{j=1}^{J} \int_{t_i}^{t_{i+1}} \mathbf{w}^{j\,T} \frac{\partial \mathbf{M}_i^j}{\partial \sigma} \mathbf{N}^j dt \\ &- \sum_{i=0}^{I-1} f_i P_i^\dagger \sum_{j=1}^{J} V^j \sum_g \frac{d\mathbf{N}^{j\,T}(t_i)}{d\sigma} \mathbf{R}_g^j \tilde{\Phi}_g^j - \sum_{i=0}^{I-1} f_i P_i^\dagger \sum_{j=1}^{J} V^j \sum_g \mathbf{N}^{j\,T}(t_i) \frac{d\mathbf{R}_g^j}{d\sigma} \tilde{\Phi}_g^j \\ &+ \left\langle \Gamma^\dagger, \frac{\partial \mathbf{B}_0}{\partial \sigma} \Phi \right\rangle + \sum_{j=1}^{J} \frac{d\mathbf{N}^{j\,T}(t_0)}{d\sigma} \left\langle \Gamma^\dagger, \frac{\partial \mathbf{B}_0}{\partial \mathbf{N}^j(t_0)} \Phi \right\rangle. \end{aligned} \quad (34)$$

The first, second, fourth and seventh terms in the RHS of Eq. (34) which include $\frac{d\mathbf{N}}{d\sigma}$ disappear if $\mathbf{w}$ is properly defined as follows. Since the fourth term in the RHS of Eq. (34) can be written as

$$-\sum_{i=0}^{I-1} \int_{t_0}^{t_I} \delta(t - t_i) f_i P_i^\dagger \sum_{j=1}^{J} V^j \frac{d\mathbf{N}^{j\,T}(t)}{d\sigma} \sum_g \mathbf{R}_g^j \tilde{\Phi}_g^j dt, \quad (35)$$

and the seventh term can be written as

$$\int_{t_0}^{t_I} \delta(t - t_0) \sum_{j=1}^{J} \frac{d\mathbf{N}^{j\,T}(t)}{d\sigma} \left\langle \Gamma^\dagger, \frac{\partial \mathbf{B}_0}{\partial \mathbf{N}^j(t_0)} \Phi \right\rangle dt, \quad (36)$$

we define the following equation for $\mathbf{w}^j$:

$$\frac{d\mathbf{w}^j}{dt} + \mathbf{M}_i^{j\,T} \mathbf{w}^j - f_i P_i^\dagger V^j \sum_g \mathbf{R}_g^j \tilde{\Phi}_g^j \delta(t - t_i) + \left\langle \Gamma^\dagger, \frac{\partial \mathbf{B}_0}{\partial \mathbf{N}^j(t_0)} \Phi \right\rangle \delta(t - t_0) = 0, \qquad (t_i \le t < t_{i+1}). \quad (37)$$

This equation can be solved backward with the final condition for $\mathbf{w}(t)$ given in Eq. (12). This equation suggests that step-type changes are given to $\mathbf{w}^j$ at the beginning of steps and sub-steps. This is what is called the *jump condition*.

By virtue of the definition of $\mathbf{w}^j$, Eq. (34) can be simplified into the following:

$$\frac{dN_k^j(t_I)}{d\sigma} = \sum_{i=0}^{I-1} \sum_{j=1}^{J} \int_{t_i}^{t_{i+1}} \mathbf{w}^{j\,T} \frac{\partial \mathbf{M}_i^j}{\partial \sigma} \mathbf{N}^j dt - \sum_{i=0}^{I-1} f_i P_i^\dagger \sum_{j=1}^{J} V^j \sum_g \mathbf{N}^{j\,T}(t_i) \frac{d\mathbf{R}_g^j}{d\sigma} \tilde{\Phi}_g^j + \left\langle \Gamma^\dagger, \frac{\partial \mathbf{B}_0}{\partial \sigma} \Phi \right\rangle. \quad (38)$$

The first, second and third terms in the RHS of Eq. (38) are referred to as the number density term, the power normalization term and the neutron flux term, respectively.

### *2.3. Implementation of fuel depletion sensitivity calculation module to deterministic reactor physics code system CBZ*

CBZ is a general-purpose reactor physics deterministic code system being developed at Hokkaido University. The CBZ code system has various modules designed to solve neutron diffusion and transport equations

based on the collision probability method, the method of characteristics, the finite-volume method, the boundary element method and the discrete-ordinate method. CBZ has other modules for reactor physics calculations such as resonance self-shielding treatment, fuel depletion and uncertainty quantification. The CBZ code system realizes various functionalities related to reactor physics and particle transport through combinations of these modules, such as direction-dependent diffusion coefficient calculations based on the method of characteristics(van Rooijen and Chiba, 2011), sensitivity calculations for fuel depletion-related quantities based on GPT for a single fuel pin(Chiba, 2013), and time-dependent delayed photon transport calculations for fast reactor fuel subassemblies(Chiba, 2014), etc. The numerical procedure for fuel depletion calculations with CBZ for multi-cell problems is briefly described below.

Resonance self-shielding calculations, *i.e.,* effective cross sections calculations, are carried out in a single pin cell model with reflective boundary conditions based on the equivalence theory. The fuel escape probabilities are evaluated by the one-term rational approximation with the optimized Bell factors and the background cross sections are evaluated by the Dancoff factor method. Resonance interference effects between different heavy nuclei are taken into account by the multiple resonance interference factors. Through these resonance self-shielding calculations, 107-group cross sections are obtained and are used for the subsequent neutron flux and fuel depletion calculations. Details of the resonance self-shielding calculation procedure of CBZ will be presented in a future paper.

The neutron flux and the generalized adjoint neutron flux are calculated by the collision probability method.

Fuel depletion calculations can be performed with arbitrary nuclide chains which can be generated automatically by a module implemented in CBZ. The choice of the nuclide chain is highly dependent on its purpose: a detailed chain consisting of over 1,000 nuclides is necessary in decay heat calculations just after reactor shutdown, and a simplified chain consisting of about several tens or a hundred of nuclides is suited for reactivity calculations during reactor operation.

Changes in nuclide number densities through fuel depletion are described by the fuel depletion equation (7), and this equation can be solved by various numerical methods. Numerical methods for solving this equation implemented in CBZ are based on the matrix exponential method, and the Mini-Max Polynomial Approximation (MMPA) method developed by Kawamoto is used to calculate the matrix exponential in our new module(Kawamoto, 2015). It should be noted that the MMPA method has the specific feature of being capable of calculating nuclide number densities at several time steps at once without an increase in computation time. This is quite suitable to the GPT calculation for fuel depletion, which requires numerical integration calculations on time interval during which integrated parameters such as $\mathbf{N}$ and $\mathbf{w}$ are significantly dependent on time. To perform accurate numerical integration for actual implementation, $\mathbf{w}$ is calculated at a finer time step than the sub-step division; the sub-step is further divided into *sub-sub-step* and $\mathbf{w}$ is calculated at every sub-sub-step. Note that the present fuel depletion module of CBZ can

be applied only to two-dimensional multicell problems with arbitrary power profiles; multi-cycle problems consisting of fresh fuel addition or fuel shuffling cannot be treated with this module.

At present, this module can calculate the sensitivities of nuclide number densities to the nuclear data after fuel depletion. Extensions of this capability to various neutronics parameters, such as the neutron multiplication factor and the spectral indices, can be easily realized(Chiba, 2013).

In addition, another comment should be made about the generalized adjoint neutron flux calculation. The generalized adjoint neutron transport equation (26) can be written as

$$\mathbf{B}^{\dagger}\Gamma^{\dagger} = \left(\mathbf{A}^{\dagger} - \frac{1}{k_{\text{eff}}}\mathbf{F}^{\dagger}\right)\Gamma^{\dagger} = S^{\dagger}, \tag{39}$$

where the subscript denoting sub-step 0 for $\mathbf{A}$, $k_{\text{eff}}$ and $\mathbf{F}$ is omitted. The solution to this equation can be written as the following Neumann series expansion(Usachev, 1964; Mitani and Kuroi, 1972):

$$\Gamma^{\dagger} = \left\{\sum_{n=0}\left(\frac{1}{k_{\text{eff}}}\mathbf{A}^{\dagger -1}\mathbf{F}^{\dagger}\right)^{n}\right\}\mathbf{A}^{\dagger -1}S^{\dagger} = \sum_{n=0}\Gamma_{n}^{\dagger}, \tag{40}$$

where

$$\begin{aligned}
\mathbf{A}^{\dagger}\Gamma_{0}^{\dagger} &= S^{\dagger}, &(41)\\
\mathbf{A}^{\dagger}\Gamma_{1}^{\dagger} &= \frac{1}{k_{\text{eff}}}\mathbf{F}^{\dagger}\Gamma_{0}^{\dagger}, &(42)\\
&\cdots &\\
\mathbf{A}^{\dagger}\Gamma_{n}^{\dagger} &= \frac{1}{k_{\text{eff}}}\mathbf{F}^{\dagger}\Gamma_{n-1}^{\dagger}, &(43)\\
&\cdots\ . &
\end{aligned}$$

Let us expand the source $S^{\dagger}$ as

$$S^{\dagger} = \sum_{i=0} a_i \mathbf{F}\Phi_{i}^{\dagger}, \tag{44}$$

where $\Phi_{i}^{\dagger}$ is the solution to the following adjoint neutron transport equation:

$$\mathbf{A}^{\dagger}\Phi_{i}^{\dagger} = \frac{1}{\lambda_i}\mathbf{F}^{\dagger}\Phi_{i}^{\dagger}. \tag{45}$$

Since the source $S^{\dagger}$ is orthogonal to $\Phi$, it can be easily derived that $a_0$ is zero and Eq. (44) is rewritten as

$$S^{\dagger} = \sum_{i=1} a_i \mathbf{F}\Phi_{i}^{\dagger}. \tag{46}$$

Since the iterative calculation based on Eqs. (41), (42) and (43) is the power iteration, it is easily understood that $\Gamma_{n}^{\dagger}$ converges to zero when $n \to \infty$. During the iterative calculation; however, numerical round-off errors affect the orthogonality and the correct convergence cannot be attained. In order to avoid this problem, the following numerical treatment is generally applied to each iteration step:

$$\mathbf{F}^{\dagger}\tilde{\Gamma}_{n} = \mathbf{F}^{\dagger}\Gamma_{n} - \frac{\left\langle \Phi, \mathbf{F}^{\dagger}\Gamma_{n}^{\dagger}\right\rangle}{\left\langle \Phi, \mathbf{F}^{\dagger}\Phi_{0}^{\dagger}\right\rangle}\mathbf{F}^{\dagger}\Phi_{0}^{\dagger}, \tag{47}$$

where $\mathbf{F}^\dagger\tilde{\Gamma}_n$ is the revised source term used in the next iteration.

In our implementation, the following different approach is taken. The source $S^\dagger$ is separated into $S_P^\dagger$ and $S_N^\dagger$, which are defined as

$$S_P^\dagger(x) = \begin{cases} S^\dagger(x) & if S^\dagger(x) > 0 \\ 0 & otherwise, \end{cases} \tag{48}$$

and

$$S_N^\dagger(x) = \begin{cases} -S^\dagger(x) & if S^\dagger(x) < 0 \\ 0 & otherwise. \end{cases} \tag{49}$$

With these two separated sources, two iterative sequences based on Eqs. (41), (42) and (43) are performed and iterative solutions $\Gamma_{P,n}^\dagger$ and $\Gamma_{N,n}^\dagger$ are obtained at the $n$th iteration from $S_P^\dagger$ and $S_N^\dagger$. Since the fundamental mode component $a_0\mathbf{F}\Phi_0^\dagger$ included in the initial sources $S_P^\dagger$ and $S_N^\dagger$ does not grow during the iteration and higher mode components decrease, $\Gamma_{P,n}^\dagger$ and $\Gamma_{N,n}^\dagger$ converge to $a_0\Phi_0^\dagger$ finally. Thus $\Gamma^\dagger$ can be obtained by the following equations if the convergence is attained at the $n'$th iteration:

$$\Gamma_P^\dagger = \sum_{n=0}^{n'} \left(\Gamma_{P,n}^\dagger - \Gamma_{P,n'}\right), \tag{50}$$

$$\Gamma_N^\dagger = \sum_{n=0}^{n'} \left(\Gamma_{N,n}^\dagger - \Gamma_{N,n'}\right), \tag{51}$$

$$\Gamma^\dagger = \Gamma_P^\dagger - \Gamma_N^\dagger. \tag{52}$$

This idea to separately treat positive and negative components in a source term was originally proposed by Yamamoto(Yamamoto, 1995). Specific features of this numerical method are that the numerical treatment described in Eq. (47) is unnecessary, negative quantity can be ignored, and no complicated convergence judgment is required for values close to zero.

## 3. Numerical procedure

In the present study, 3×3 and 5×5 multi-cell problems consisting of PWR-simulated $UO_2$ and MOX pin cells with the white boundary conditions are considered. Geometric specifications and initial nuclide number densities of these fuel cells are taken from the reference(Katakura, 2004). Sensitivities of nuclide number densities of uranium-235, plutonium-239, americium-241 and gadolinium-156 after 1,000-day depletion with respect to several nuclear data are calculated. Neutron flux is normalized to $3.2\times10^{14}$[/cm$^2$·s] at the concerned fuel cell. A nuclide depletion chain consisting of 138 fission product nuclides, which is optimized for light water reactor reactivity calculations(Chiba, 2015), is employed.

In addition to sensitivities of number densities of these specific nuclides, nuclear data-induced uncertainties which can be obtained with the sensitivities and covariance data of neutron-nuclide reaction cross

sections are calculated. In this calculation, covariance data of capture, fission and (n,2n) cross sections of the following 16 nuclides are considered; U-234, -235, -238, Np-237, Pu-238, -239, -240, -241, -242, Am-241, -243, Cm-242, -243, -244, -245 and -246. These covariance data are taken from JENDL-4.0(Shibata, 2011).

## 4. Numerical results

### *4.1. Verification*

The functionality of GPT-based sensitivity calculations of nuclide number densities is verified through comparisons with sensitivity calculations with direct numerical differentiation. Sensitivities are calculated on a 3×3 multi-cell problem, as depicted in **Fig. 1**. Sensitivities to uranium-238 capture cross section at pin 1 ($UO_2$) and pin 2 (MOX), and those to uranium-235 fission cross section at pin 3 ($UO_2$) are shown in **Figs. 2** to **4**. In these figures, "Ref." corresponds to reference sensitivities calculated by the direct calculations and "GPT" corresponds to sensitivities calculated by the GPT functionality newly implemented into CBZ. Sensitivities (multiplied by 0.25) per lethargy are displayed in these figures because lethargy width of each energy group above 1.8554 eV is 0.25 in the present calculations. As generally good agreement between these two sensitivities is obtained, it can be concluded that the newly implemented GPT functionality is well verified. There are some differences in sensitivities of plutonium-239 and americium-241 number densities to uranium-238 capture cross sections between 10 and 100 eV. The reason of these differences are not clear at present, but the absolute values of these sensitivity differences are not significant.

### *4.2. Effect of neighboring fuels in 3×3 multi-cell problem*

In order to see the effects of neighboring fuels on fuel depletion sensitivities, sensitivities of nuclide number densities in the same $UO_2$ fuel cell are calculated with different arrangements of surrounding fuel cells. The central fuel pin with four different arrangements is shown in **Fig. 5**. All the neighboring fuel pins are $UO_2$ in case 1 and contributions of the MOX cell increase in cases 2, 3 and 4.

First sensitivities of uranium-235 number densities to several cross sections are shown in **Fig. 6**. Neutron flux energy spectra become harder as the contribution of the MOX cell becomes larger. Differences in energy profiles of sensitivities to uranium-235 fission and capture cross sections can be explained by the shifting of neutron flux spectra. Sensitivities to plutonium isotope cross sections become larger as the contribution of the MOX cell becomes larger. It is interesting to note that sensitivities to uranium-238 capture cross sections become small when the MOX contribution is large. Generally, sensitivity of uranium-235 number density to uranium-238 capture cross section is positive. When the uranium-238 capture cross section increases, it increases plutonium-239 production which enhances neutron flux energy spectrum hardening. This results in the reduction of neutron reaction rates with uranium-235 and moderates depletion of uranium-235. Because this effect is relatively large if the neutron flux energy spectrum is soft, this sensitivity takes larger values in case 1 than other cases.

Next, sensitivities of plutonium-239 number densities to several cross sections are shown in **Fig. 7**. Although the trend observed in sensitivities to uranium-238 capture cross sections is similar to that in Fig. 6, the following different interpretation is possible. It is well known that the conversion ratio of uranium-238 to plutonium-239 becomes large if the neutron flux energy spectrum is hard. The large conversion ratio is equivalent to the fact that the cancellation between plutonium-239 production and plutonium-239 consumption is less significant. Therefore, the effect of the increase in uranium-238 capture reactions to the net production of plutonium-239 is large if this cancellation is significant. This is because sensitivities of plutonium-239 number density to uranium-238 capture cross section become large when the contribution of the MOX cell is small, as in case 1.

**Table 1** shows nuclear data-induced uncertainties of nuclide number densities after fuel depletion. Some dominated nuclear data-induced uncertainties are also shown. Uncertainties in Gadolinium-156 number density mainly come via neutron flux spatial and energy distributions. Non-negligible differences among different cell arrangements are observed in the nuclear data-induced uncertainties.

### *4.3. Effect of neighboring fuels in 5×5 multi-cell problem*

To see the effects of distance from different fuel pins on fuel depletion sensitivities, sensitivities of nuclide number densities of the same $UO_2$ fuel cell under the same depletion conditions are calculated at different pin positions. A 5×5 multi-cell, in which a MOX fuel pin is located at the center, is shown in **Fig. 8**. Fuel pins labeled 1, 2 and 3 are $UO_2$ fuel pins, and the sensitivities of these pins are compared.

Sensitivities of gadolinium-156 number densities to several cross sections are shown in **Fig. 9**. Whereas slight differences among different pin positions are observed, dependence of sensitivities on pin position, *i.e.*, distance from different fuel pin, is generally negligible. On sensitivities of uranium-235, plutonium-239 and americium-241 number densities, the differences among different pin positions are much smaller.

**Table 2** shows nuclear data-induced uncertainties of nuclide number densities after fuel depletion. Dependence of the nuclear data-induced uncertainties on pin position is negligible.

## 5. Concluding remarks

A new functionality of fuel depletion sensitivity calculations has been developed as one module in a deterministic reactor physics code system CBZ. This is based on the generalized perturbation theory for fuel depletion problems. The theory for fuel depletion problems with a multi-layer depletion step division scheme has been described in detail. Numerical techniques employed in actual implementation have also been provided. Verification calculations have been carried out for a 3×3 multi-cell problem consisting of two different fuel pins. It has been shown that sensitivities of nuclide number densities after fuel depletion calculated by the new module agree well with reference sensitivities calculated by direct numerical differentiation. To demonstrate the usefulness of the new module, fuel depletion sensitivities in different multi-cell

arrangements have been compared with one another, and non-negligible differences have been observed. Nuclear data-induced uncertainties of nuclide number densities obtained with the calculated sensitivities have also been compared. In addition, sensitivities in a 5×5 multi-cell problem have been calculated, and it has been shown that the dependence of sensitivities on distance from different fuel pins is negligible.

The following further developments are now planned: extension of GPT to fuel depletion calculations with the predictor-corrector method for lattice systems including gadolinium-bearing fuel pins, and replacement of the collision probability module by the method of characteristic module for large systems such as fuel assemblies.

## Acknowledgements

This work received funding from the nuclear regulatory authority of Japan. The authors are grateful to Mr. Takanori Kajihara of Hokkaido University for his support for this study.

## References

Chiba, G., Tsuji, M., Narabayashi, T., 2013. Uncertainty quantification of neutronic parameters of light water reactor fuel cells with JENDL-4.0 covariance data, J. Nucl. Sci. Technol., 50, 751-760.

Chiba, G., Tsuji, M., Narabayashi, T., 2014. Photon transport effect on intra-subassembly thermal power distribution in fast reactor, Ann. Nucl. Energy, 65, 41-46.

Chiba, G., Tsuji, M., Narabayashi, T., Ohoka, Y., Ushio, T., 2015. Important fission product nuclides identification method for simplified burnup chain construction, J. Nucl. Sci. Technol., 52, 953-960.

Katakura, J., Kataoka, M., Suyama, K., Jin, T., Ohki, S., 2004. A set of ORIGEN2 cross section libraries based on JENDL-3.3 library: ORLIBJ33, JAERI-Data/Code 2004-015, Japan Atomic Energy Research Institute.

Kawamoto, Y., Chiba, G., Tsuji, M., Narabayashi, T., 2015. Numerical solution of matrix exponential in burn-up equation using mini-max polynomial approximation, Ann. Nucl. Energy, 80, 219-224.

Mitani, H., Kuroi, H., 1972. Sensitivity coefficient of integral data and generalized perturbation method, JAERI-M 4760, Japan Atomic Energy Research Institute. (in Japanese)

Shibata, K., Iwamoto, O., Nakagawa, T., Iwamoto, N., Ichihara, A., Kunieda, S., Chiba, S., Furutaka, K., Otuka, N., Ohsawa, T., Murata, T., Matsunobu, H., Zukeran, A., Kamada, S., Katakura, J., 2011. JENDL-4.0: a new library for nuclear science and engineering, J. Nucl. Sci. Technol., 48, 1-30.

Takeda, T., Umano, T., 1985. Burnup sensitivity analysis in a fast breeder reactor - Part I: Sensitivity calculation method with generalized perturbation theory, Nucl. Sci. Eng., 91, 1-10.

Usachev, L.N., 1964. Perturbation theory for the breeding ratio and for other number ratios pertaining to various reactor processes, J. Nucl. Energy Parts A/B, 18, 571-583.

van Rooijen, W.F.G., Chiba, G., 2011. Diffusion coefficients for LMFBR cells calculated with MOC and Monte Carlo methods, Ann. Nucl. Energy, 38, 133-144.

Williams, M.L., 1979. Development of depletion perturbation theory for coupled neutron/nuclide fields, Nucl. Sci. Eng., 70, 20-36.

Yamamoto, T., 1995. Optimization study on the diffusion synthetic acceleration algorithm in three-dimensional discrete ordinate transport, J. Nucl. Sci. Technol., 32, 804-812.

Table 1: Nuclear data-induced uncertainties of nuclide number densities after fuel depletion in a 3×3 multi-cell problem

| | | Case 1 | Case 2 | Case 3 | Case 4 |
|---|---|---|---|---|---|
| Uranium-235 | Total | 1.10 | 0.63 | 0.61 | 0.45 |
| | U-238(n,$\gamma$) | 1.04 | 0.46 | 0.41 | 0.25 |
| | Pu-240(n,$\gamma$) | 0.24 | 0.35 | 0.37 | 0.31 |
| Plutonium-239 | Total | 2.26 | 1.90 | 1.87 | 1.67 |
| | U-238(n,$\gamma$) | 2.21 | 1.83 | 1.79 | 1.61 |
| Americium-241 | Total | 5.34 | 4.36 | 4.20 | 3.71 |
| | Am-241(n,$\gamma$) | 4.20 | 3.30 | 3.10 | 2.59 |
| | Pu-240(n,$\gamma$) | 2.01 | 2.12 | 2.17 | 2.12 |
| | Pu-241(n,$\gamma$) | 1.53 | 1.11 | 1.03 | 0.87 |
| | U-238(n,$\gamma$) | 1.66 | 1.13 | 1.08 | 0.94 |
| Gadolinium-156 | Total | 0.65 | 0.65 | 0.72 | 0.80 |
| | U-238(n,$\gamma$) | 0.54 | 0.22 | 0.19 | 0.07 |
| | Pu-240(n,$\gamma$) | 0.08 | 0.45 | 0.55 | 0.66 |

Table 2: Nuclear data-induced uncertainties of nuclide number densities after fuel depletion in a 5×5 multi-cell problem

| | | Pin 1 | Pin 2 | Pin 3 |
|---|---|---|---|---|
| Uranium-235 | Total | 1.00 | 1.02 | 1.04 |
| | U-238(n,$\gamma$) | 0.92 | 0.96 | 1.04 |
| Plutonium-239 | Total | 2.22 | 2.22 | 2.22 |
| | U-238(n,$\gamma$) | 2.16 | 2.16 | 2.17 |
| Americium-241 | Total | 5.14 | 5.22 | 5.24 |
| | Am-241(n,$\gamma$) | 4.01 | 4.11 | 4.12 |
| | Pu-240(n,$\gamma$) | 2.09 | 2.04 | 2.03 |
| | Pu-241(n,$\gamma$) | 1.43 | 1.47 | 1.48 |
| | U-238(n,$\gamma$) | 1.55 | 1.59 | 1.60 |
| Gadolinium-156 | Total | 0.64 | 0.63 | 0.63 |
| | U-238(n,$\gamma$) | 0.50 | 0.51 | 0.51 |

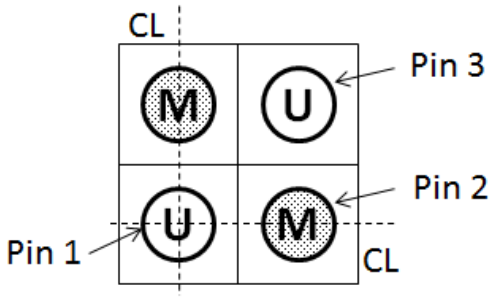


Figure 1: 3×3 multi-cell problem for verification calculations. “U” and “M” stand for $UO_2$ and MOX fuel cells, respectively.

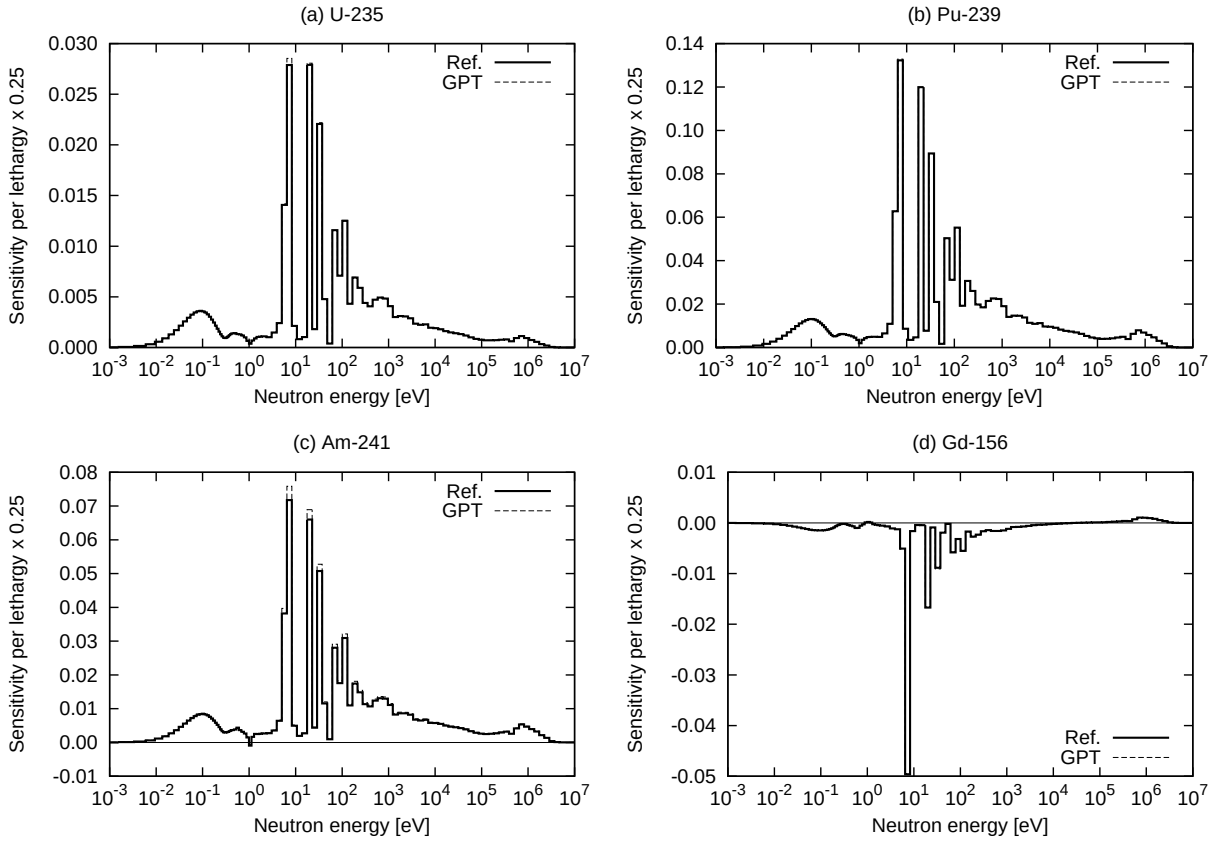


Figure 2: Sensitivities of nuclide number densities after fuel depletion to uranium-238 capture cross section in a $3 \times 3$ multi-cell problem (pin 1)

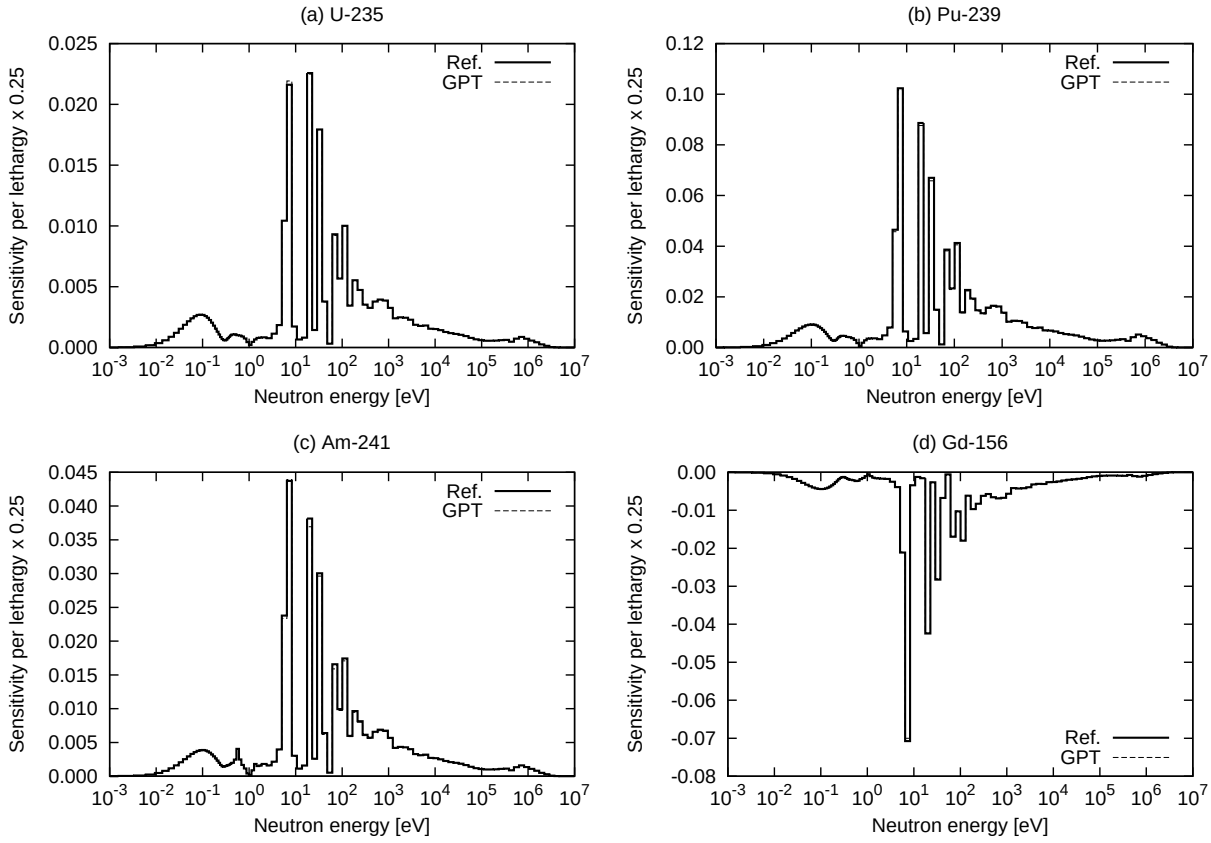


Figure 3: Sensitivities of nuclide number densities after fuel depletion to uranium-238 capture cross section in a $3 \times 3$ multi-cell problem (pin 2)

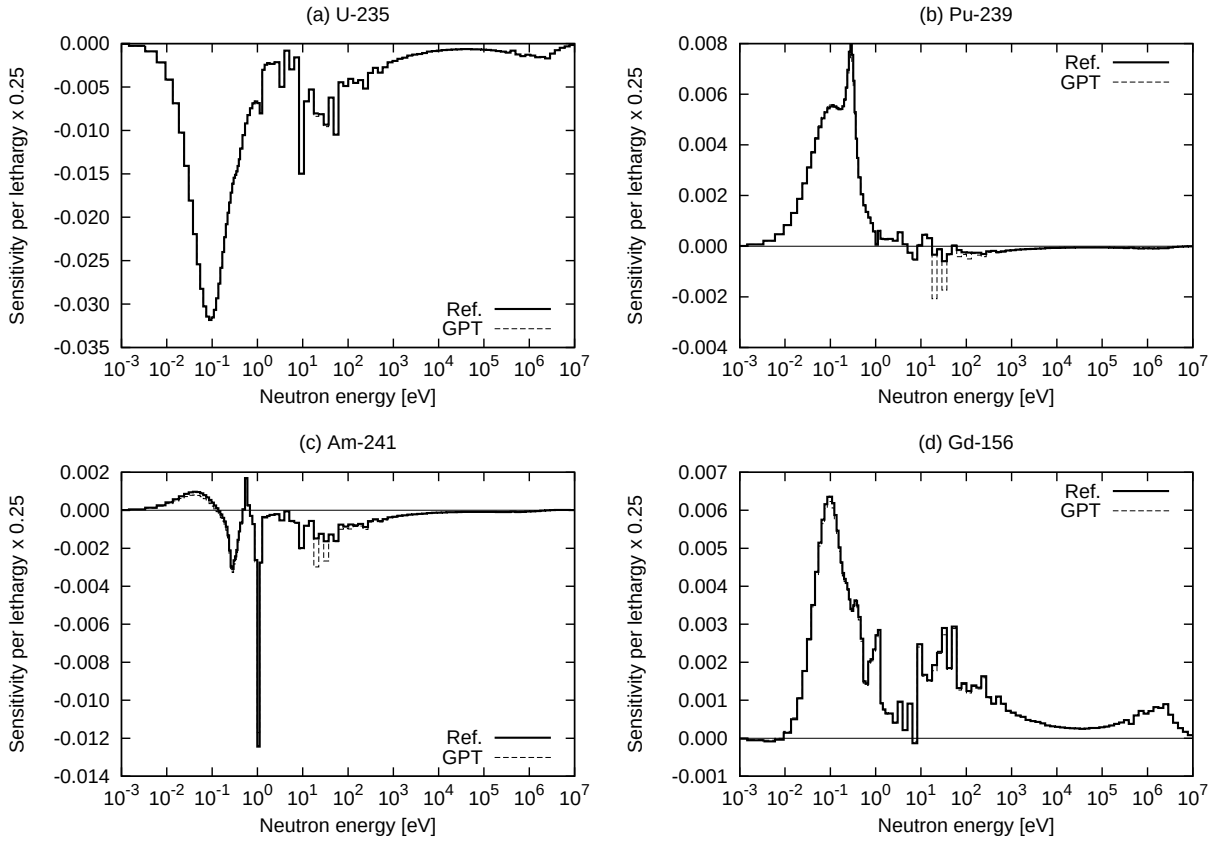


Figure 4: Sensitivities of nuclide number densities after fuel depletion to uranium-235 fission cross section in a $3 \times 3$ multi-cell problem (pin 3)

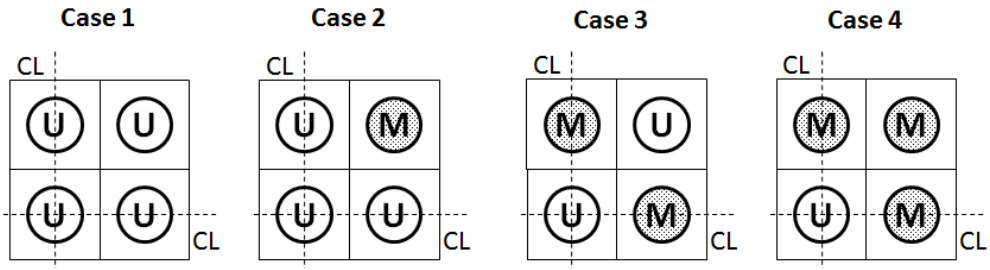


Figure 5: 3×3 multi-cell problem with different arrangements

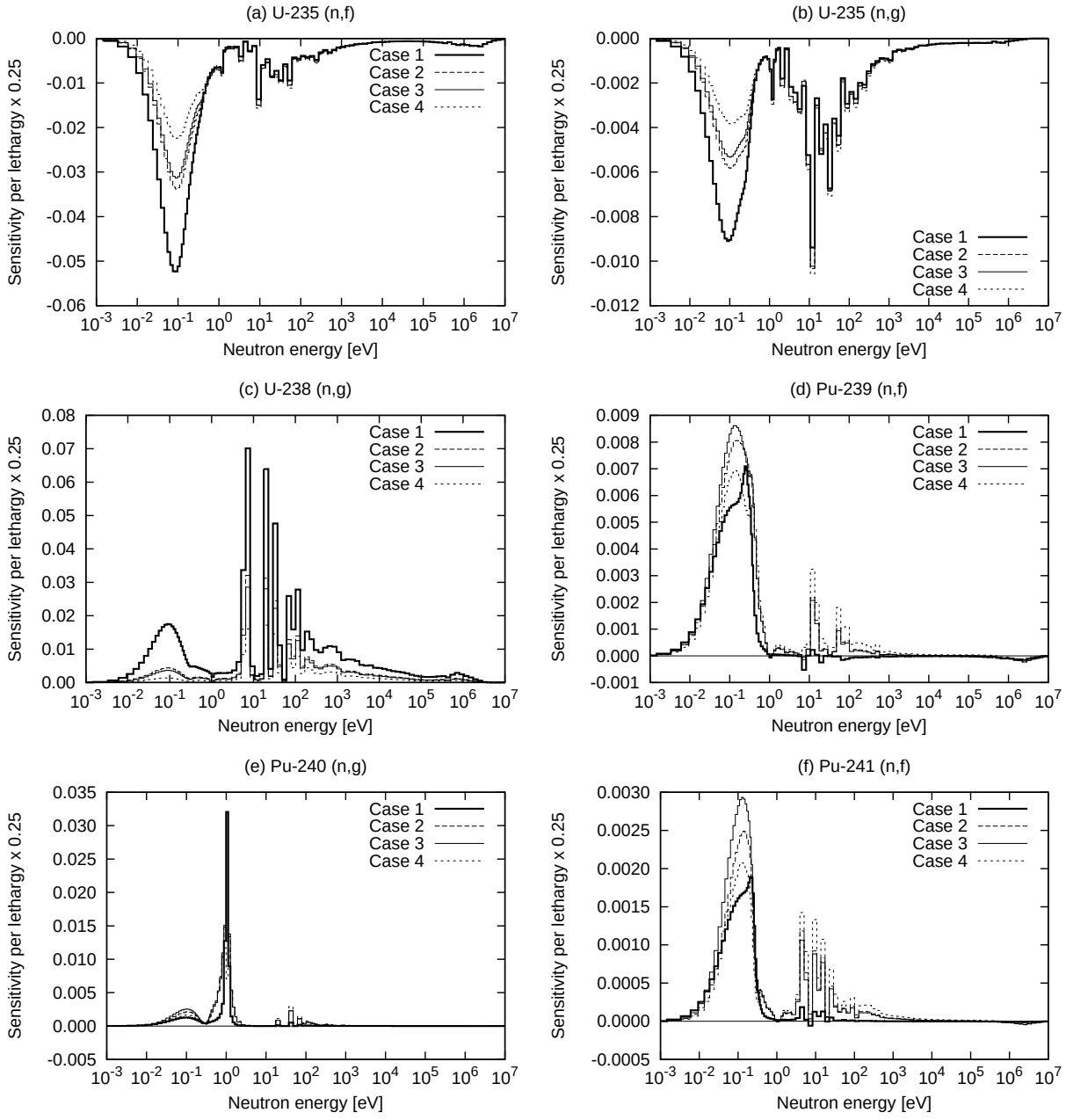


Figure 6: Sensitivities of uranium-235 number densities after fuel depletion to several cross sections in a 3×3 multi-cell problem

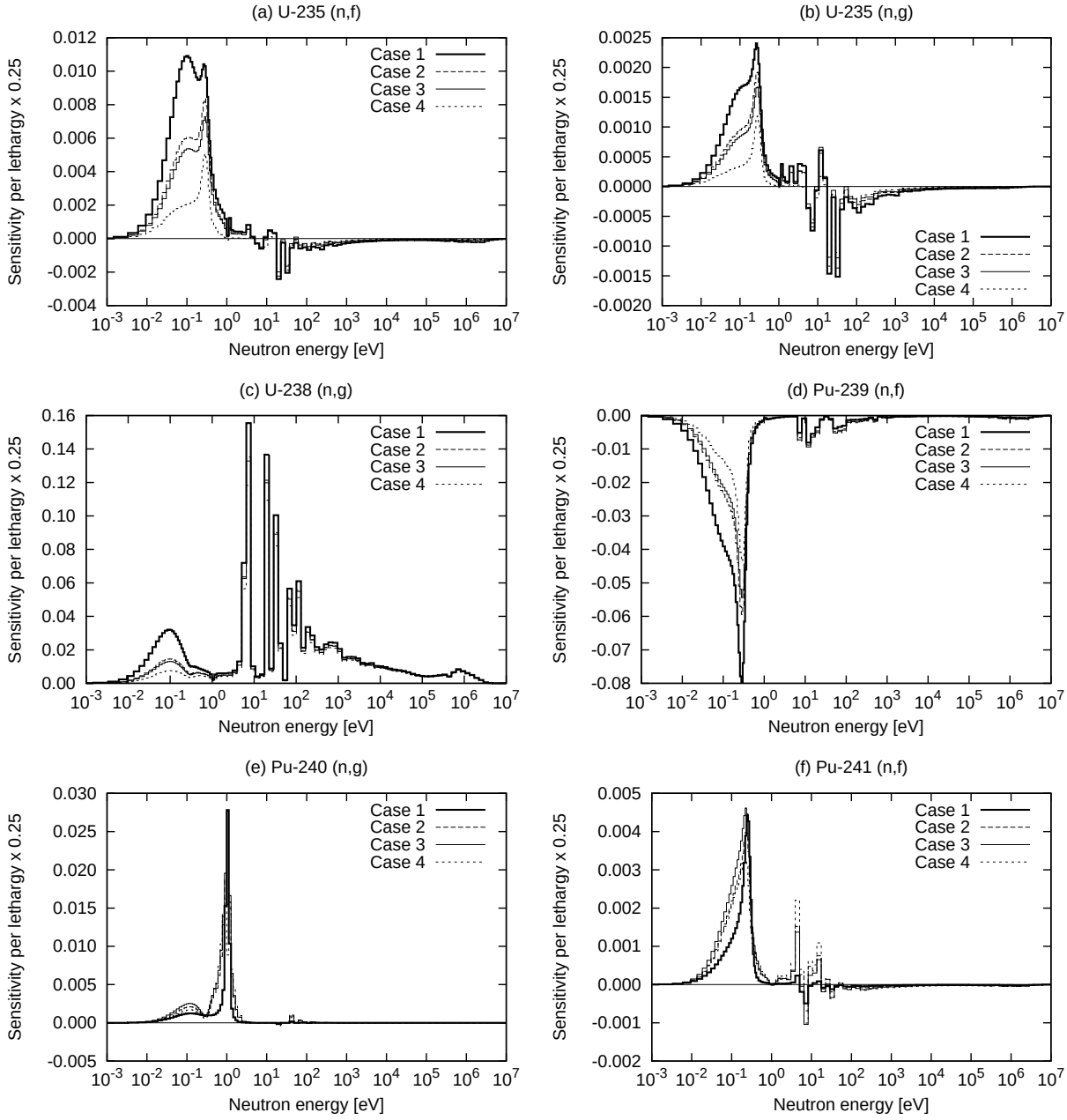


Figure 7: Sensitivities of plutonium-239 number densities after fuel depletion to several cross sections in a 3×3 multi-cell problem

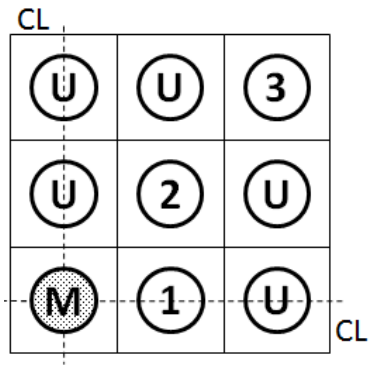


Figure 8: 5×5 multi-cell problem

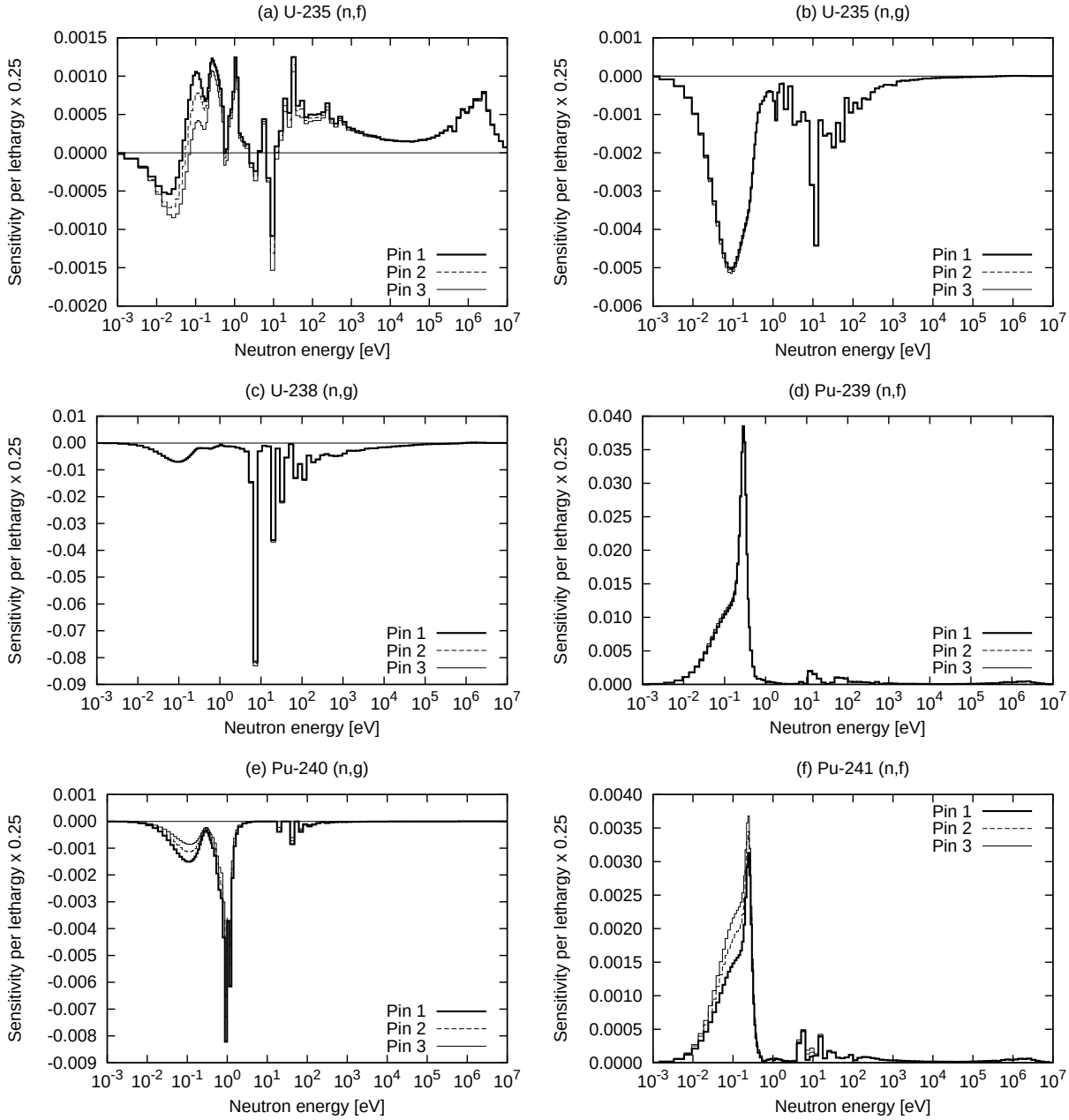


Figure 9: Sensitivities of gadolinium-156 number densities after fuel depletion to several cross sections in a 5×5 multi-cell problem

## List of Figure Captions